

## Alkali-Metal Spin Maser

W. Chalupczak and P. Josephs-Franks

National Physical Laboratory, Hampton Road, Teddington TW11 0LW, United Kingdom

(Received 10 February 2015; published 16 July 2015)

Quantum measurement is a combination of a read-out and a perturbation of the quantum system. We explore the nonlinear spin dynamics generated by a linearly polarized probe beam in a continuous measurement of the collective spin state in a thermal alkali-metal atomic sample. We demonstrate that the probe-beam-driven perturbation leads, in the presence of indirect pumping, to complete polarization of the sample and macroscopic coherent spin oscillations. As a consequence of the former we report observation of spectral profiles free from collisional broadening. Nonlinear dynamics is studied through exploring its effect on radio frequency as well as spin noise spectra.

DOI: 10.1103/PhysRevLett.115.033004

PACS numbers: 32.80.Xx, 03.65.Ta, 07.55.Ge

**Introduction.**—It is generally recognized that a probe introduces perturbations into a quantum system it monitors [1]. Mostly this has a detrimental effect on the performance of the quantum measurement and a number of probe (backaction) perturbation-evasion schemes have been proposed and demonstrated [2–4].

This Letter explores the probe perturbation in experiments with thermal alkali-metal atomic samples [5]. Thermal samples of alkali-metal atoms are extensively explored in the context of atomic sensors [4,6,7] and quantum-information processing [8]. Traditionally in this type of experiment, the atomic collective spin state is read-out by an off-resonant linearly polarized probe beam. Figure 1 shows such a spin state, with spin operator,  $\hat{F} = \sum_{i=1}^N \hat{f}^{(i)}$ , where  $N$  is the number of atoms and  $\hat{f}^{(i)}$  is the total angular momentum operator of the  $i$ th atom [9,10]. Interrogation is realized by Faraday-type rotation of light polarization measurements [11]. The linearly polarized light ( $\vec{E}_p$ ) couples to the atomic ground state through the tensor ac polarizability  $\alpha_2$  [thus a single-spin Hamiltonian, without the scalar part of the tensor light shift  $H_{\text{TLS}} = \alpha_2(\vec{E}_p \cdot \hat{F})^2$ ], therefore collective atomic spin dynamics will in general exhibit a nonlinear character [12].

In this Letter we demonstrate probe-laser-beam generated nonlinear spin dynamics through its effects on radio frequency [13] as well as spin-noise spectra [14]. We present two novel phenomena that are observed in different probe-beam-power regimes. In the low-power regime we show that the nonlinear perturbation can increase the observed coherence relaxation time. The decoherence of the ground-state coherences in alkali-metal atomic samples is determined by spin-exchange collisions (SEC) between atoms, collisions of the atoms with cell walls, and inhomogeneity of the magnetic and optical (probe) fields. Standard methods to reduce relaxation rely on antirelaxation coating of the cell walls [15], coherence transfer [16,17], and optical pumping into the stretched state [18,19], i.e., the state with maximum or minimum

quantum number  $m$ . We show that the combination of probe perturbation with indirect pumping [20] can effectively build up atomic collective spin, in particular, dynamically trap the entire atomic population in the stretched state [creating maximum imbalance, known as orientation, in population distribution among Zeeman sublevels, Fig. 1(a)]. Consequently, we report observation of a spectral profile free from collisional broadening with relaxation times up to 10 sec. In the high-probe-beam-power regime the tensor interaction with atoms in the stretched state creates a torque that tilts atomic collective spin [Fig. 1(b)] and leads to precession, analogous to that observed in a spin maser [21,22]. In this way the very same perturbation mechanism that contributes to the spin buildup, also generates the system evolution (coherence oscillation). That is, it creates a pumping and rephasing mechanism. Consequently, we demonstrate macroscopic oscillation of the atomic spin, with an extremely long lifetime that extends beyond the standard limit [23]. This arises from the nonlinear spin dynamics that drives

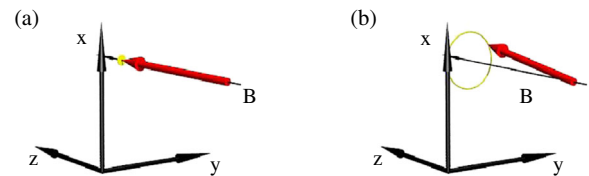


FIG. 1 (color online). Atomic collective spin (red arrow): component along the direction of the magnetic field, quantization axis, (marked with a black arrow) is set by the population imbalance among the Zeeman sublevels of the ground state, while the components orthogonal to the magnetic field represent ground state coherences [9]. An indirect pumping orients atomic spins along the  $z$  axis. (a) Mean value of  $F_x, F_y$  spin components is equal to zero. Instantaneous fluctuations of  $F_x, F_y$  are represented by the yellow circle. (b) Probe-beam nonlinear perturbation creates the torque that tilts the atomic collective spin (nonzero mean value of  $F_x, F_y$ ). As a result, spin precession around the magnetic field is observed.

pumping and rephasing processes and is in contrast to the standard optical pumping, which extends the lifetime of the coherence through orientation buildup as well as contributes to its shortening (dephasing) [24]. Finally, the same tensor interaction that generates spin precession when acting on an atom in the stretched state can lead also to one atom spin squeezing [25–27]. In our system, we verify the presence of the coherence (alignment) oscillations that can produce the squeezing within a single atom.

*Experimental setup.*—The experimental investigations are completed based on radio frequency (rf) spectroscopy, in which a scan of the rf magnetic-field frequency yields the center frequencies, widths, and amplitudes of the Zeeman coherences, and spin-noise spectroscopy, where precession of  $F_x, F_y$  collective spin components in the offset magnetic field is monitored (Fig. 2). The measurement instrumentation is described in detail in Ref. [20]; here only the key elements of the setup are introduced. The Cs vapor is housed in an antirelaxation-coated glass cell. The ambient magnetic field is suppressed by the use of five layers of mu metal (shielding factor of  $10^6$ ). An offset static magnetic field of  $1.5 \mu\text{T}$  (corresponding to Larmor frequency,  $\nu_L = 5.3 \text{ kHz}$ ) is created by two axial solenoids. The atomic vapor is optically pumped by a circularly polarized laser beam, 20 mm in diameter, frequency locked close to the  $F = 3 \rightarrow F' = 2$  of the cesium  $D_2$  line (Fig. 2). A second, 16 mm in diameter, probe beam is linearly polarized and is frequency stabilized to the  $F = 4 \rightarrow F' = 5$  transition, and then frequency shifted by a set of acousto-optic modulators to 960 MHz blue detuned (Fig. 2). The rf field is created by a set of coils and oscillates along the y direction. The probe light transmitted through the cell is analyzed by a polarimeter, and the resulting signal is processed by a lock-in amplifier and signal analyzer.

*Indirect pumping.*—The pumping within the  $F = 4$  ground-state Zeeman sublevels is achieved as a consequence of a direct pumping within the  $F = 3$  manifold,

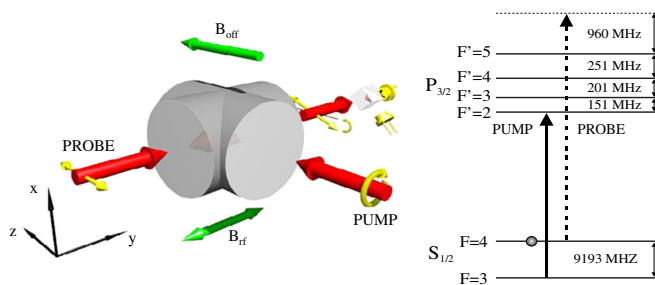


FIG. 2 (color online). Geometry of the experiment. Circularly polarized laser beam (solid arrow in level scheme) pumps cesium atoms along the offset magnetic field  $B_{\text{off}}$ . Magnetic sublevels (in rf spectroscopy measurements) are coupled by the resonant rf field oscillating in the y direction. The collective spin state is detected by analyzing the polarization state of the off-resonant probe beam propagating along the y axis (dashed arrow in level scheme).

off-resonant pumping from  $F = 3$  to  $F = 4$  and SEC state selective relaxation [20]. Pumping to the stretched state reduces SEC relaxation (light narrowing), since SEC between atoms in such states do not introduce relaxation, as the total angular momentum must be conserved in this process [18,19]. For the stretched states, this leaves no opportunity for the colliding atoms to move to any other states. Implementation of indirect optical pumping ensures that the observed linewidths are not affected by pump laser power broadening [9].

*Nonlinear spin dynamics.*—Atomic polarization evolution in the presence of a magnetic field  $B_z$  and an electric field  $E_p$  [ $H_{\text{int}} = H_B + H_{\text{TLS}} = g_F \mu_B B_{\text{off}} \hat{F}_z + \alpha_2 (\vec{E}_p \cdot \hat{F})^2$ ] has been the subject of a number of theoretical [25] and experimental [12,28,29] studies. To summarize, atomic polarization exposed to a static magnetic and off-resonant ac electric field will oscillate (e.g., alignment-orientation conversion) with the period of the oscillations equal to  $(2\pi/\Delta\nu_{\text{TLS}}) = [3/2\hbar(2F-1)]\alpha_2|E_p|^2$ ,  $\Delta\nu_{\text{TLS}}$  equal to line separation generated by the tensor light shift [25]. For  $\Delta\nu_{\text{TLS}}$  smaller than the coherence relaxation rate, the latter will determine the atomic spin dynamics (low-probe-beam-power regime) while for  $\Delta\nu_{\text{TLS}}$  bigger than the coherence relaxation rate (high-probe-beam-power regime), nonlinear perturbation will dominate the system dynamic [12].

*Low-power regime: light narrowing.*—For  $\Delta\nu_{\text{TLS}}$  smaller than the coherence relaxation rate, SEC and indirect pumping dominate system dynamics and pumping into the stretched state [Fig. 1(a)] is enhanced by the nonlinear perturbation process. The signature of this enhancement is light narrowing of the spectral profile linewidth [18,19]. In order to demonstrate variation of the linewidth across a wide range of probe-beam powers the following section presents analysis of the rf spectral profile linewidth. As a consequence of the fluctuation-dissipation theorem the general character of rf spectroscopy and spin-noise spectroscopy signals is the same, and indeed we have observed the effect of line narrowing in rf as well as spin-noise spectra. Figure 3 shows the dependence of the rf spectral linewidth (full width at half maximum,  $\Delta\nu$ ) on probe-beam power recorded with an atomic density  $1.2 \times 10^{11} \text{ cm}^{-3}$  (blue dots) [30]. Values of  $\Delta\nu_{\text{TLS}}$  are plotted with purple solid line [31]. The linewidth of the profile does not change with probe-beam power in the power range 0.1–10  $\mu\text{W}$  (we refer to that linewidth value as  $\Delta\nu_0$ ). This particular value of  $\Delta\nu_0$  results from indirect pumping and coherence transfer between pairs of Zeeman sublevels of the  $F = 4$  ground state [17]. It is important to stress that  $\Delta\nu_0$  (3 Hz) reflects the reduced value (from 5.6 Hz) caused by the high population (80% of atoms) of the stretched state. Above 10  $\mu\text{W}$   $\Delta\nu$  gradually decreases until it reaches a minimum around 0.67 mW (where  $\Delta\nu_{\text{TLS}} \sim \Delta\nu_0$ ). The dashed (orange) line in Fig. 3 shows the linewidth value defined by collisions with the cell walls (1.1 Hz). The fact that the recorded linewidths reach that value indicates that the light

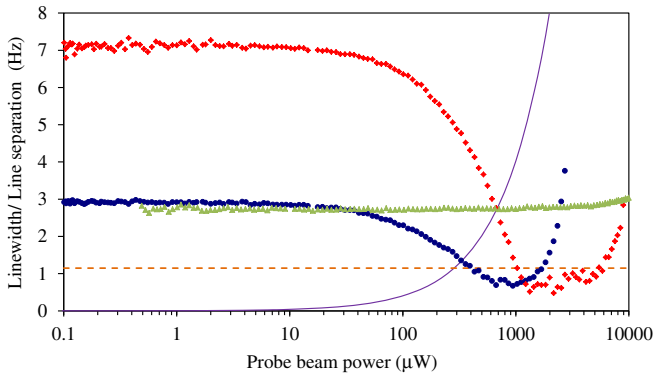


FIG. 3 (color online). Linewidth of the rf signal dependence on probe-beam power recorded at two atomic densities  $1.2 \times 10^{11} \text{ cm}^{-3}$  (blue dots) and  $2.4 \times 10^{11} \text{ cm}^{-3}$  (red diamonds). The probe beam is tuned 960 MHz away from resonance. The solid (purple) line shows the line separation produced by the tensor light shift measured with the well-resolved spectra at Larmor frequency 520 kHz. Green triangles represent the rf signal linewidth power dependence recorded at atomic density  $1.2 \times 10^{11} \text{ cm}^{-3}$  with the probe beam tuned 11 GHz away from resonance. Dashed (orange) line shows the linewidth value defined by collisions with the cell walls.

narrowing mechanism eliminates SEC relaxation. When  $\Delta\nu_{\text{TLS}} > \sqrt{2}\Delta\nu_0$  (probe light powers bigger than 2 mW) an increase of the linewidth is observed resulting from the splitting of the line into eight components.

In order to verify that the minimum linewidth recorded in our measurement represents spin-exchange-free relaxation we have repeated the measurement with the atomic sample at a higher density. Figure 3 (red diamonds) shows the dependence of rf signal linewidth on probe-beam power recorded at atomic density  $2.4 \times 10^{11} \text{ cm}^{-3}$ . It is worth pointing out that the  $\Delta\nu(2.4 \times 10^{11} \text{ cm}^{-3})$  has same generic dependence as  $\Delta\nu(1.2 \times 10^{11} \text{ cm}^{-3})$  on probe-beam power: the minimum is reached for  $\Delta\nu_{\text{TLS}} = \Delta\nu_0(2.4 \times 10^{11} \text{ cm}^{-3}) = 7.2 \text{ Hz}$ ; while  $\Delta\nu(2.4 \times 10^{11} \text{ cm}^{-3})$  starts to increase when  $\Delta\nu_{\text{TLS}} > \sqrt{2}\Delta\nu_0(2.4 \times 10^{11} \text{ cm}^{-3})$ . Described observations prove that the relaxation dynamics of the system is governed by the difference between nonlinear perturbation ( $\Delta\nu_{\text{TLS}}$ ) and relaxation rates ( $\Delta\nu_0$ ). Although  $\Delta\nu_0(2.4 \times 10^{11} \text{ cm}^{-3})$  is more than twice of  $\Delta\nu_0(1.2 \times 10^{11} \text{ cm}^{-3})$ , the minimum value for both cases is the same.

Resolution of the linewidth shown (Fig. 3) is limited by the measurement bandwidth and the minimum value of  $\Delta\nu$  shown in Fig. 3 does not reflect intrinsic coherence times. The decoherence rate manifests itself in relaxation as well as in buildup of the signal. In order to demonstrate atomic coherence times for  $\Delta\nu_{\text{TLS}} \sim \Delta\nu_0$  we have recorded the buildup of the atomic spin signal (the rf field is turned off) after the probe light is turned on. Figure 4 shows the temporal evolution of the polarization-rotation signal generated by the atomic spin components orthogonal to the offset magnetic field after turning on the probe light. The

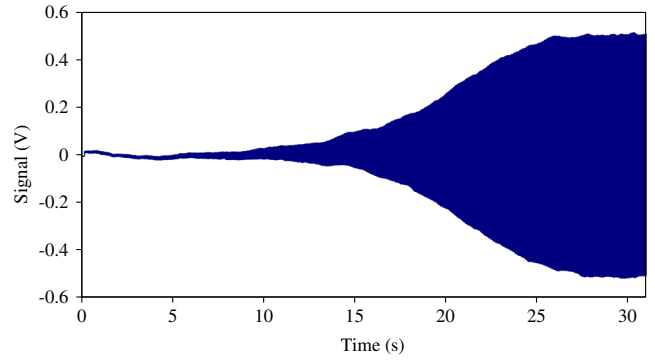


FIG. 4 (color online). Spin oscillation signal ( $\nu_L = 5.3 \text{ kHz}$ ) after the probe-beam light is turned on recorded at atomic density  $1.2 \times 10^{11} \text{ cm}^{-3}$ , probe power around 0.7 mW.

rise time of the signal on the order of 10 sec was observed for the probe light powers around 0.7 mW, while above that power a gradual decrease in rise time has been detected (See Supplemental Material at [32] for FFT spectrum of the spin oscillations).

The strength of the probe-beam coupling to the atomic ground state ( $\alpha_2$ ) decreases with the square of the laser frequency detuning from the resonance [12]. We have verified that the effect has resonant character by performing measurements with the probe laser tuned 11 GHz away from resonances involving  $F = 4$  ground-state Zeeman sublevels (green triangles in Fig. 3). We have verified the essential character of the probe-beam profile homogeneity across the entire cell aperture by observation of the linewidth probe-power dependence for a beam with lower diameter, which showed the reduced effect of narrowing [33].

*High-power regime: spin maser.*—For the  $\Delta\nu_{\text{TLS}} \sim \Delta\nu_0$  combination of the tensor interactions and indirect pumping traps, the atomic population is in a polarized (oriented) state [Fig. 1(a)]. For  $\Delta\nu_{\text{TLS}} > \Delta\nu_0$  nonlinear perturbation dominates the system dynamics. It initiates the transfer from orientation to alignment [25]. In the first stage of that process probe light couples every other Zeeman sublevel of the ground state, which corresponds to atomic coherences oscillating at  $2\nu_L$ . Figure 5 shows the dependence of the amplitude of the spin-noise spectroscopy signal on probe-beam power. It confirms the presence of the spin signal oscillating at  $2\nu_L$  in the probe-beam-power range 800–2000  $\mu\text{W}$  (light-blue squares in Fig. 5). Generation of that coherence (the component of the spin orthogonal to the magnetic field direction) is equivalent to the torque that tilts the atomic spin [Fig. 1(b)] and initiates the precession of the collective spin around the magnetic field direction. The blue dots (red diamonds) in Fig. 5 represent probe-beam-power dependence of the amplitudes of the spin spectra recorded at  $\nu_L = 5.3 \text{ kHz}$  with atomic density  $1.2 \times 10^{11} (2.4 \times 10^{11}) \text{ cm}^{-3}$ . In both cases we observed a dramatic change of spin amplitude for probe power above

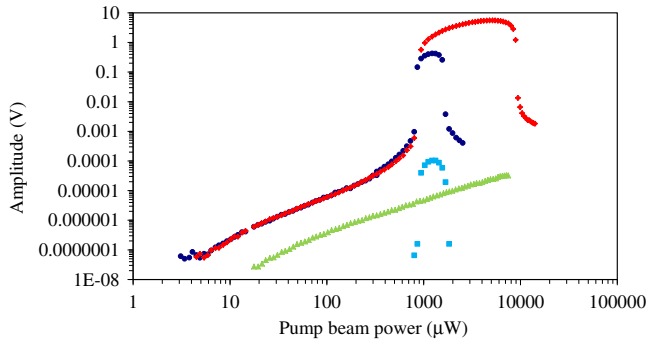


FIG. 5 (color online). Dependence of the amplitude of the spin-noise spectroscopy oscillating at 5.3 kHz on the probe-beam power recorded at two atomic densities of  $1.2 \times 10^{11} \text{ cm}^{-3}$  (blue dots) and  $2.4 \times 10^{11} \text{ cm}^{-3}$  (red diamonds). Green triangles represent the power dependence recorded with the probe beam tuned 11 GHz away from resonance. Light-blue squares show the probe-beam-power dependence of the amplitude of the spin noise spectroscopy signal oscillating at 10.6 kHz recorded at  $1.2 \times 10^{11} \text{ cm}^{-3}$ .

a value corresponding to complete polarization of the atomic sample ( $\Delta\nu_{\text{TLS}} \sim \Delta\nu_0$ ) [34]. The observed increase of the spin spectrum amplitude results from transition between the cases a and b in Fig. 1, i.e., start-up of the oscillation of the atomic spin initiated by nonlinear probe perturbation. The effect is analogous to the spin maser in noble gas samples, where the magnetic field from a pick-up coil (probe) tilts the sample magnetization with respect to the direction of the magnetic field [21,22]. The magnetic field from the pick-up coil initiates and reinforces the oscillation of the magnetization. Analogously, the nonlinear spin dynamics initiates (through tilt) and reinforces (through the spin build-up mechanism) the oscillation of the coherence. In other words, pumping mechanism is synchronized with coherence generation and provides a rephasing mechanism for spin oscillation, which enables observation of a coherence lifetime longer than for the case of standard optical pumping [23]. Additionally, it confirms that nonlinear spin dynamics leads to a buildup of the atomic collective spin regardless of its direction with respect to the static magnetic field. In particular, spin oriented along the magnetic field [low-power regime, Fig. 1(a)] and also the precessing spin [high-power regime, Fig. 1(b)] both benefit from the mechanism. An abrupt decrease of the amplitude at higher probe powers in Fig. 5 is due to tensor light shift that causes coherences, coupling different pairs of Zeeman sublevels, to oscillate at different frequencies. To verify the essential role of tensor interaction we recorded probe-beam-power dependence of the spin-spectra amplitude with the probe-beam frequency detuned 11 GHz away from resonance (green triangles in Fig. 5, atomic density  $1.2 \times 10^{11} \text{ cm}^{-3}$ ). The data set shows no amplitude changes present in other data sets in Fig. 5. Comparison of the amplitudes recorded at two densities

(within the same power range, i.e., 1028–1327  $\mu\text{W}$ , spectral profiles have same linewidth) confirms the nonlinear character of the spin dynamics (scales with the square of the atomic density).

*Entanglement.*—It has been pointed out that the nonlinear coupling,  $[\sim\alpha_2(\vec{E}_p \cdot \hat{F})^2]$ , is equivalent to single axis twisting and can produce spin squeezing [35]. The measurement reported in [27] demonstrated that the protocol, involving transfer of the entire atomic population into a stretched state and generation of atomic coherences oscillating at  $2\nu_L$ , produces indeed spin squeezing within individual atoms. Results presented in Fig. 3 (the entire population in the stretched state) and Fig. 5 (spin oscillation at  $2\nu_L$ ) demonstrate a presence of these two key components in our system.

*Conclusions.*—The long lifetime of the atomic ground-state coherences is an essential factor in practical implementations of quantum-enhanced metrology such as atomic clocks [36,37], magnetometers [38], gyroscopes [39], quantum memory [40], as well as spin squeezing [4], quantum nondemolition measurements [41], precision measurements of fundamental symmetries [42], and cosmology (search for domain walls formed by axionlike fields [43]). Significant progress has been achieved in the design and implementation of various protocols that prolong that time [44,45]. This Letter has presented an approach based on the combination of the probe-beam generated perturbation with indirect pumping. The uniqueness of the presented technique is in (i) the novel pumping method, (ii) the degree of linewidth narrowing, and (iii) the wide range of experimental conditions in which it is applicable. Implementation of probe-beam driven spin oscillation in an atomic magnetometer could potentially provide us with a tool for electric-dipole-moment measurements [46], as well as dc alkali-metal magnetometers operating in a nonzero magnetic field environment [47].

The work was funded by the U.K. Department for Business, Innovation and Skills as part of the National Measurement System Programme and U.K. MOD Science and Technology Programme (via Dstl Contract NO. DSTL/AGR/00315/01).

- 
- [1] V. B. Braginsky and F. Ya. Khalili, *Quantum Measurement* (Cambridge University Press, Cambridge, England, 1992).
  - [2] V. Shah, G. Vasilakis, and M. V. Romalis, *Phys. Rev. Lett.* **104**, 013601 (2010).
  - [3] G. Vasilakis, V. Shah, and M. V. Romalis, *Phys. Rev. Lett.* **106**, 143601 (2011).
  - [4] W. Wasilewski, K. Jensen, H. Krauter, J. J. Renema, M. V. Balabas, and E. S. Polzik, *Phys. Rev. Lett.* **104**, 133601 (2010).
  - [5] Experiments are conducted in cesium with thermal atomic velocity distribution, vapor temperature range  $20^\circ$ – $50^\circ$ . In

- general, temperatures in experiments with alkali-metal atoms range between  $20^{\circ}$ – $200^{\circ}$ .
- [6] X. Xia, A. Ben-Amar Baranga, D. Hoffman, and M. V. Romalis, *Appl. Phys. Lett.* **89**, 211104 (2006).
- [7] C. N. Johnson, P. D. D. Schwindt, and M. Weisend, *Appl. Phys. Lett.* **97**, 243703 (2010); C. N. Johnson, P. D. D. Schwindt, and M. Weisend, *Phys. Med. Biol.* **58**, 6065 (2013).
- [8] N. J. Cerf, G. Leuchs, and E. S. Polzik, *Quantum Information with Continuous Variables of Atoms and Light* (Imperial College Press, London, 2007).
- [9] B. Julsgaard, J. Sherson, J. L. Sorensen, and E. S. Polzik, *J. Opt. B* **6**, 5 (2004).
- [10] J. M. Geremia, J. K. Stockton, and H. Mabuchi, *Phys. Rev. A* **73**, 042112 (2006).
- [11] Y. Takahashi, K. Honda, N. Tanaka, K. Toyoda, K. Ishikawa, and T. Yabuzaki, *Phys. Rev. A* **60**, 4974 (1999).
- [12] G. A. Smith, S. Chaudhury, A. Silberfarb, I. H. Deutsch, and P. S. Jessen, *Phys. Rev. Lett.* **93**, 163602 (2004).
- [13] D. Budker and D. F. Jackson Kimball, *Optical magnetometry* (Cambridge University Press, Cambridge, England, 2013).
- [14] S. A. Crooker, D. G. Rickel, A. V. Balatsky, and D. L. Smith, *Nature (London)* **431**, 49 (2004).
- [15] M. V. Balabas, T. Karaulanov, M. P. Ledbetter, and D. Budker, *Phys. Rev. Lett.* **105**, 070801 (2010).
- [16] W. Happer and A. C. Tam, *Phys. Rev. A* **16**, 1877 (1977).
- [17] W. Chalupczak, P. Josephs-Franks, B. Patton, and S. Pustelny, *Phys. Rev. A* **90**, 042509 (2014).
- [18] S. Appelt, A. B. Baranga, A. R. Young, and W. Happer, *Phys. Rev. A* **59**, 2078 (1999).
- [19] I. M. Savukov and M. V. Romalis, *Phys. Rev. A* **71**, 023405 (2005).
- [20] W. Chalupczak, R. M. Godun, P. Anielski, A. Wojciechowski, S. Pustelny, and W. Gawlik, *Phys. Rev. A* **85**, 043402 (2012).
- [21] M. G. Richards, B. P. Cowan, M. F. Secca, and K. Machin, *J. Phys. B* **21**, 665 (1988).
- [22] T. E. Chupp, R. J. Hoare, R. L. Walsworth, and Bo Wu, *Phys. Rev. Lett.* **72**, 2363 (1994).
- [23] I. M. Savukov, S. J. Seltzer, M. V. Romalis, and K. L. Sauer, *Phys. Rev. Lett.* **95**, 063004 (2005).
- [24] The fourth term in Eq. (10) in Ref. [18] describes reduction of SEC relaxation through atomic polarization (orientation), while the third term shows damping of the precessing spin due to the projection onto a pure (stretched) state.
- [25] S. M. Rochester, M. P. Ledbetter, T. Zigdon, A. D. Wilson-Gordon, and D. Budker, *Phys. Rev. A* **85**, 022125 (2012).
- [26] S. Chaudhury, S. Merkel, T. Herr, A. Silberfarb, I. H. Deutsch, and P. S. Jessen, *Phys. Rev. Lett.* **99**, 163002 (2007).
- [27] T. Fernholz, H. Krauter, K. Jensen, J. F. Sherson, A. S. Sorensen, and E. S. Polzik, *Phys. Rev. Lett.* **101**, 073601 (2008).
- [28] M. C. Kuntz, R. C. Hilborn, and A. M. Spencer, *Phys. Rev. A* **65**, 023411 (2002).
- [29] D. Budker, D. F. Kimball, S. M. Rochester, and V. V. Yashchuk, *Phys. Rev. Lett.* **85**, 2088 (2000).
- [30] The rf spectrum profile consists of 8 overlapping resonances representing degenerate or nearly degenerate coherences between pairs of neighboring Zeeman sublevels of  $F = 4$  ground state. Each resonance has the same linewidth [17]. We characterize the profile linewidth with a single parameter  $\Delta\nu$ , namely, the width of the line representing coherence coupled to a stretched state.
- [31] Measurement of the tensor light shift produced line separation has been done at high offset field,  $\nu_L = 520$  kHz [a similar measurement has been reported in W. Chalupczak, A. Wojciechowski, S. Pustelny, and W. Gawlik, *Phys. Rev. A* **82**, 023417 (2010)]. In that condition the nonlinear component of the Zeeman effect (about 60 Hz) produces a well-resolved spectrum. This allows accurate measurement of the line separation dependence on probe-beam power. The solid line in Fig. 3 represents a linear fit to that dependence.
- [32] See Supplemental Material at <http://link.aps.org/supplemental/10.1103/PhysRevLett.115.033004> for Fourier transform of the spin oscillations.
- [33] K. Jensen, V. M. Acosta, J. M. Higbie, M. P. Ledbetter, S. M. Rochester, and D. Budker, *Phys. Rev. A* **79**, 023406 (2009).
- [34] The probe power, for which the increase of the signal amplitude in Fig. 5 is observed changes with atomic density differently than suggested in the discussion of Fig. 3. It can result from the fact that the conditions for steady-state maser oscillation [e.g., Eq. (4a) in [21]; Eq. (3) in [22]] is set not only by the ratio of the perturbation rate to the coherence relaxation rate but also includes the factor related to instantaneous and equilibrium sample polarizations, i.e., polarization in the absence of the perturbation, which for this measurement is a function of the atomic density [20].
- [35] M. Kitagawa and M. Ueda, *Phys. Rev. A* **47**, 5138 (1993).
- [36] H. G. Robinson and C. E. Johnson, *Appl. Phys. Lett.* **40**, 771 (1982).
- [37] Y.-Y. Jau, A. B. Post, N. N. Kuzma, A. M. Braun, M. V. Romalis, and W. Happer, *Phys. Rev. Lett.* **92**, 110801 (2004).
- [38] D. Budker and M. V. Romalis, *Nat. Phys.* **3**, 227 (2007).
- [39] T. W. Kornack, R. K. Ghosh, and M. V. Romalis, *Phys. Rev. Lett.* **95**, 230801 (2005).
- [40] B. Julsgaard, J. Sherson, J. I. Cirac, J. Flurasek, and E. S. Polzik, *Nature (London)* **432**, 482 (2004).
- [41] A. Kuzmich, L. Mandel, and N. P. Bigelow, *Phys. Rev. Lett.* **85**, 1594 (2000).
- [42] W. C. Griffith, M. D. Swallows, T. H. Loftus, M. V. Romalis, B. R. Heckel, and E. N. Fortson, *Phys. Rev. Lett.* **102**, 101601 (2009).
- [43] M. Pospelov, S. Pustelny, M. P. Ledbetter, D. F. Jackson Kimball, W. Gawlik, and D. Budker, *Phys. Rev. Lett.* **110**, 021803 (2013).
- [44] L. Viola and S. Lloyd, *Phys. Rev. A* **58**, 2733 (1998).
- [45] G. Arrad, Y. Vinkler, D. Aharonov, and A. Retzker, *Phys. Rev. Lett.* **112**, 150801 (2014).
- [46] T. Inoue, T. Furukawa, A. Yoshimi, Y. Ichikawa, M. Chikamori, Y. Ohtomo, M. Tsuchiya, N. Yoshida, H. Shirai, M. Uchida, K. Suzuki, T. Nanao, H. Miyatake, H. Ueno, Y. Matsuo, T. Fukuyama, and K. Asahi, *Hyperfine Interact.* **220**, 59 (2013).
- [47] W. Gawlik, L. Krzemien, S. Pustelny, D. Sangla, J. Zachorowski, M. Graf, A. O. Sushkov, and D. Budker, *Appl. Phys. Lett.* **88**, 131108 (2006); S. Pustelny, A. Wojciechowski, M. Gring, M. Kotyrba, J. Zachorowski, and W. Gawlik, *J. Appl. Phys.* **103**, 063108 (2008).